Electronic Supplementary Material (ESI) for Materials Chemistry Frontiers.

Supporting Information for

"Tuning the exchange-coupling effect in raspberry-like γ-Fe_2O_3@CoO nanoparticles engineered through single variation of the surfactant concentration in the synthesis process"

Clémentine Bidaud[a], David García-Soriano[a], Elena H. Sánchez[b], Jean-Marc Grenèche[c], José A. De Toro[b], Maria Varela[d], Mónica Dhanjani[a], Alberto Bollero[a,*], Gorka Salas[a,*]

[a] IMDEA Nanociencia, C/ Faraday 9, Cantoblanco, 28049, Madrid, Spain.

[b] Instituto Regional de Investigación Científica Aplicada (IRICA) and Departamento de Física Aplicada, Universidad de Castilla-La Mancha, 13071 Ciudad Real, Spain.

[c] Institut des Molécules et Matériaux du Mans (UMR CNRS 6283), Le Mans Université, Avenue Olivier Messiaen, 72085 Le Mans Cedex, France.

[d] Departamento de Física de Materiales & Instituto Pluridisciplinar, Universidad Complutense de Madrid, Madrid 28040, Spain.

Corresponding authors: A. Bollero (alberto.bollero@imdea.org) and G. Salas (gorka.salas@imdea.org)

The supporting material here provided contains figures with the following information intended to support results and discussion provided in the main manuscript:

(a) Transmission Electron Microscopy (TEM) images:

- Figures S1 to S6 show TEM micrographs of γ-Fe_2O_3@CoO NPs synthesized with an oleic acid-to-cobalt molar ratio OAc/Co = 0/1, 1/1, 2/1, 3/1, 5/1 and 8/1. It is worth remarking -as explained in the main manuscript- that the cobalt concentration remains unchanged in the synthesis and it is only the surfactant (oleic acid) content that is varied. These images demonstrate that an increase in the concentration of the surfactant leads to an increased number of the CoO satellites grown onto the surface of the γ-Fe_2O_3 nanoparticles.
- Figure S7 shows successful growth of cobalt oxide particles when using surfactant but no iron oxide seeds (OAc/Co molar ratio used: 3/1).

(b) Magnetic characterization:

- Figure S8 shows the derivative of ZFC measurements (included in Figure 7.a in the main manuscript) with temperature used to obtain the average T_B for γ-Fe_2O_3 seeds and γ-Fe_2O_3 @CoO NP with molar ratios OAc/Co = 3/1 and 8/1.
- Figure S9 shows the hysteresis loop measured at 5 K after field-cooling (50 kOe) for the γ-Fe_2O_3 @CoO nanoparticles synthesized with a molar ratio OAc/Co = 3/1.

(c) Results from ICP-OES measurements for different OAc/Co ratios shown in Table S1.

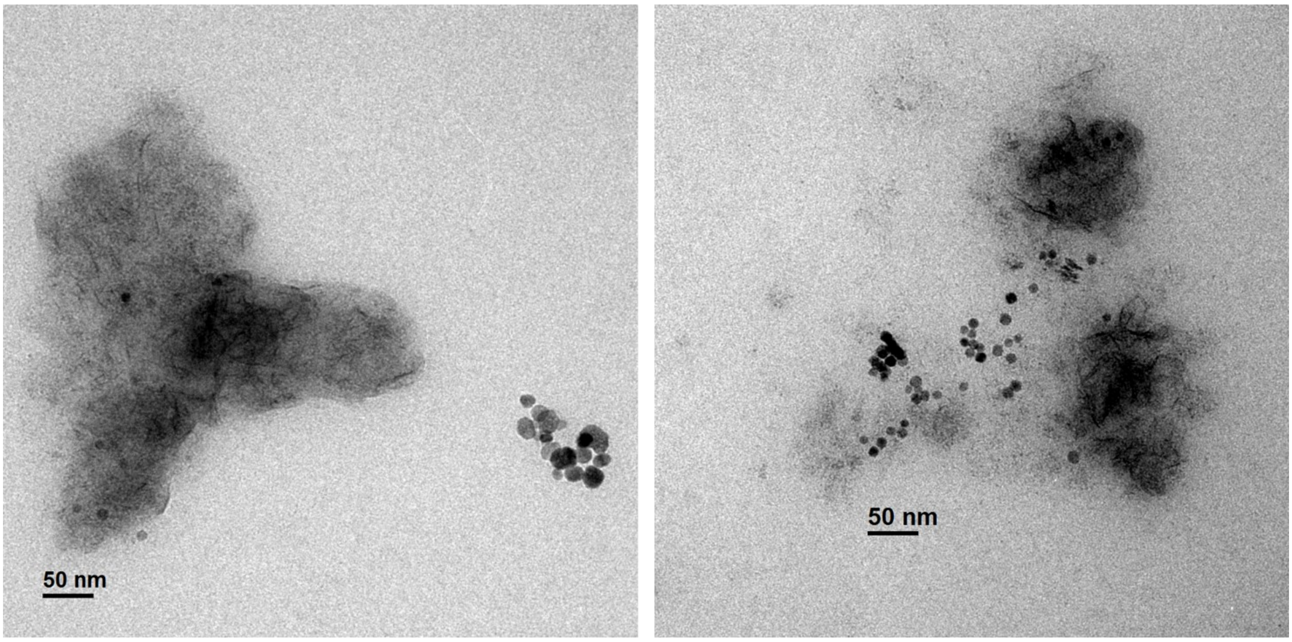

Figure S1. TEM micrographs of γ-Fe_2O_3@CoO NPs synthesized with a molar ratio OAc/Co = 0/1.

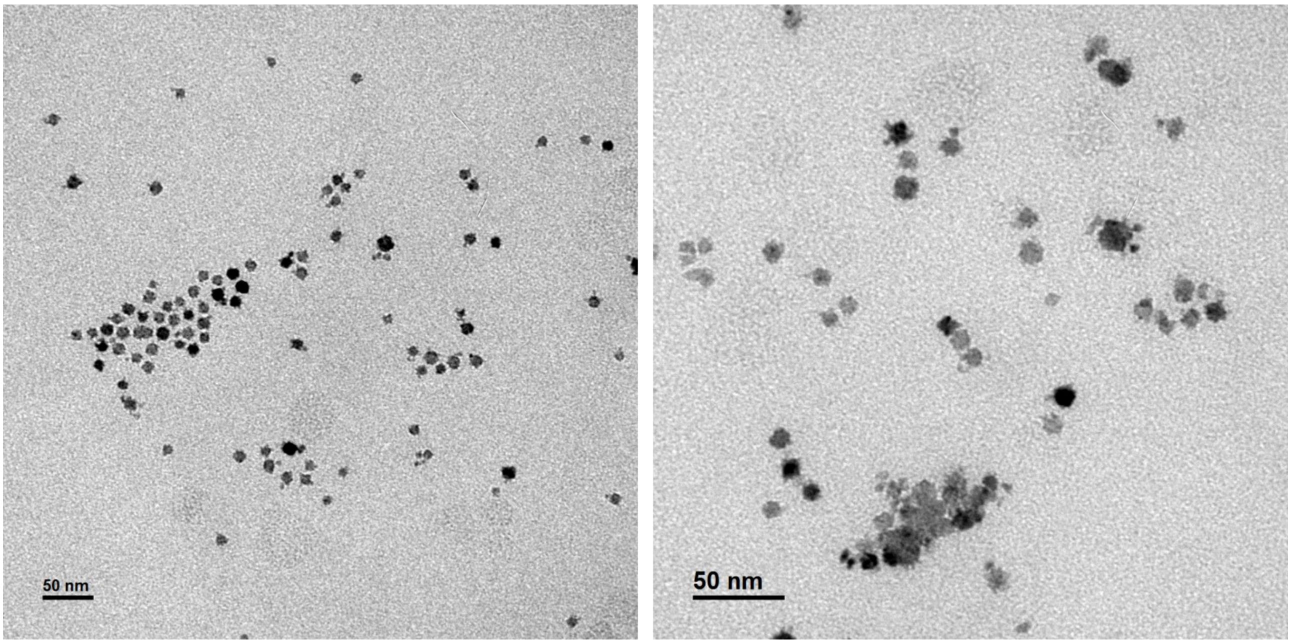

Figure S2. TEM micrographs of γ-Fe_2O_3@CoO NPs synthesized with a molar ratio OAc/Co = 1/1.

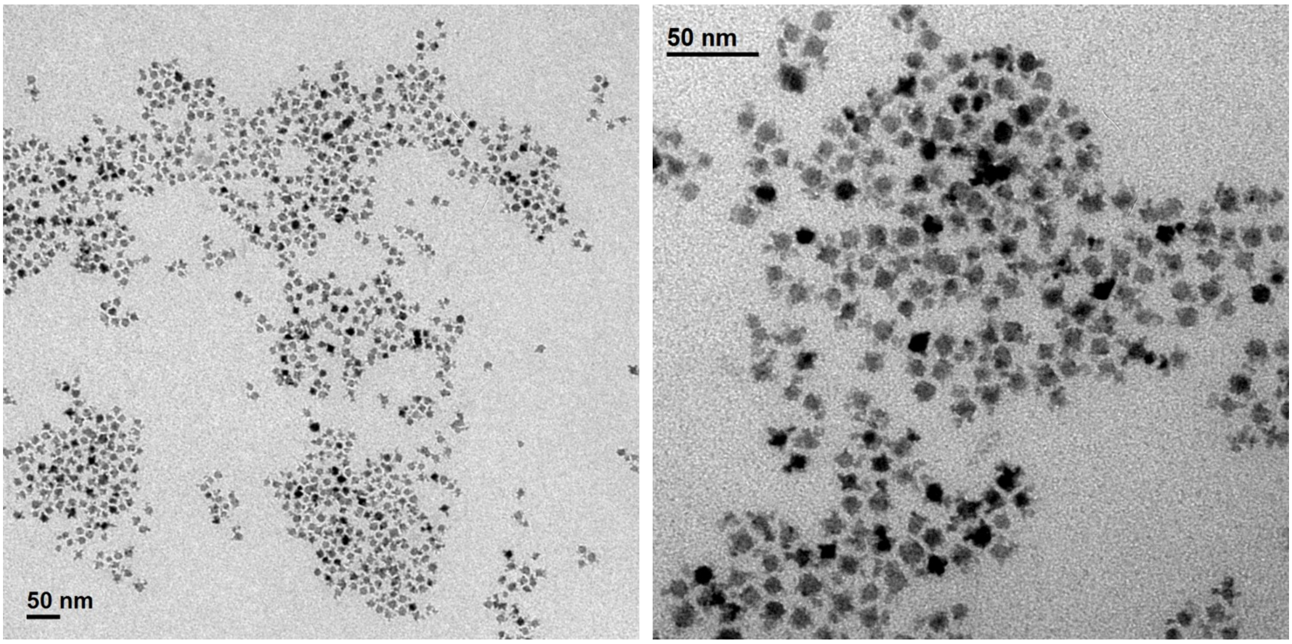

Figure S3. TEM micrographs of γ-Fe_2O_3@CoO NPs synthesized with a molar ratio OAc/Co = 2/1.

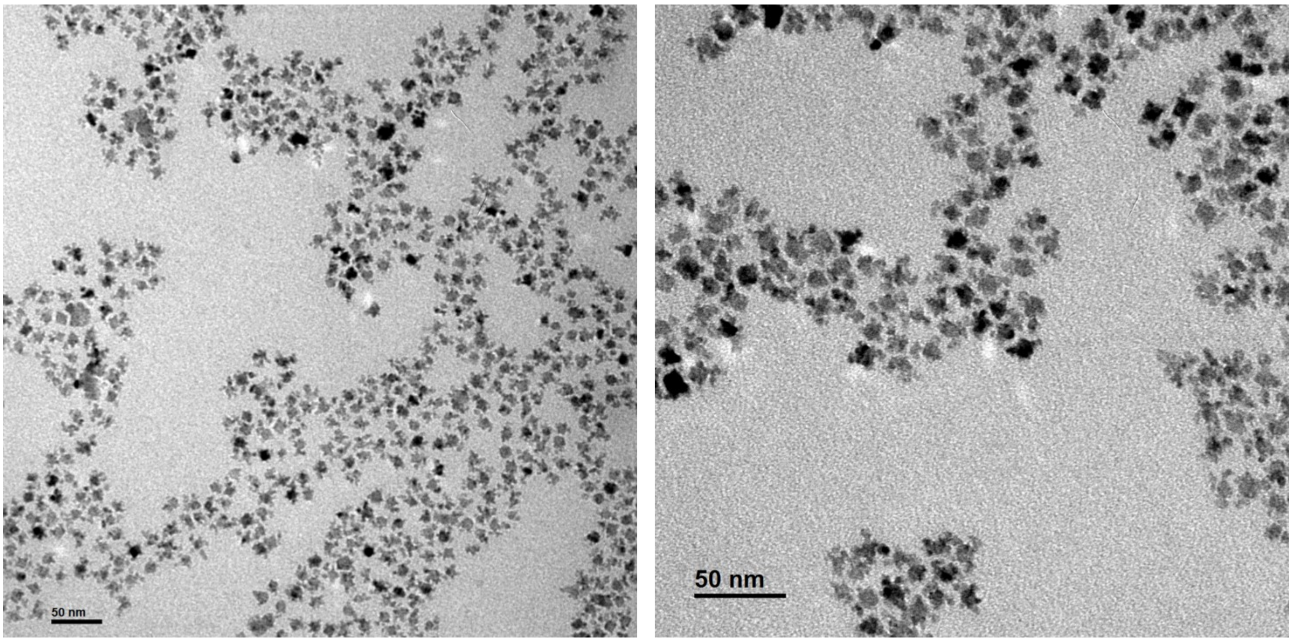

Figure S4. TEM micrographs of γ-Fe_2O_3@CoO NPs synthesized with a molar ratio OAc/Co = 3/1.

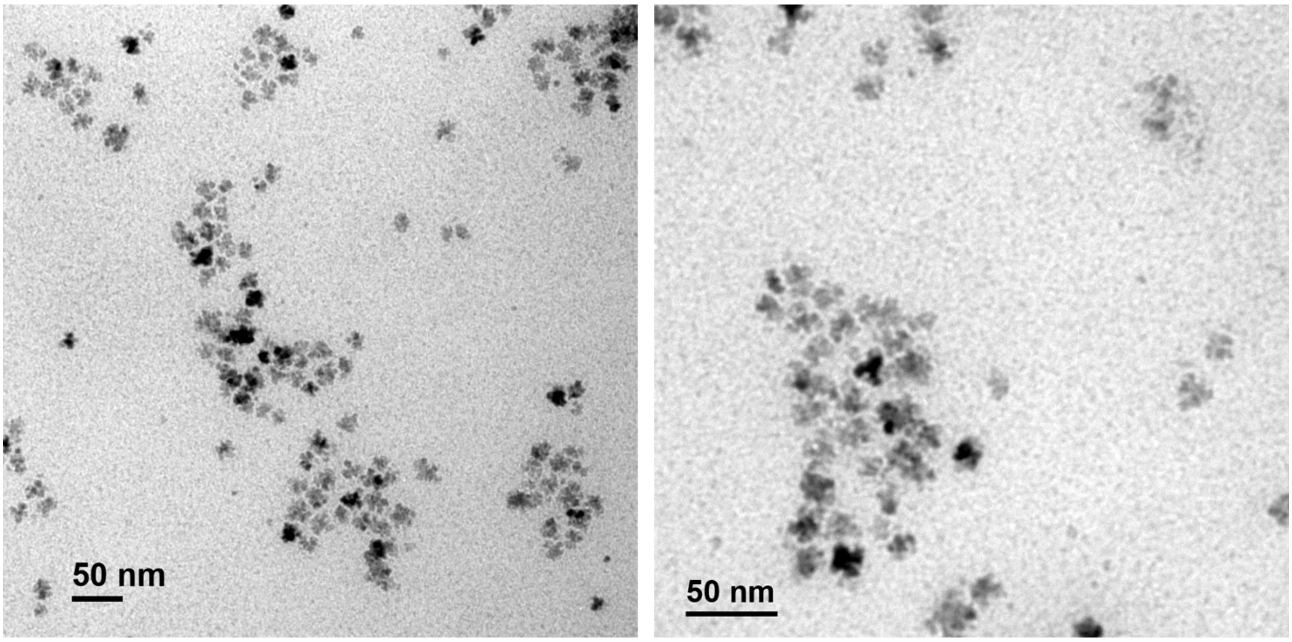

Figure S5. TEM micrographs of γ-Fe_2O_3@CoO NPs synthesized with a molar ratio OAc/Co = 5/1.

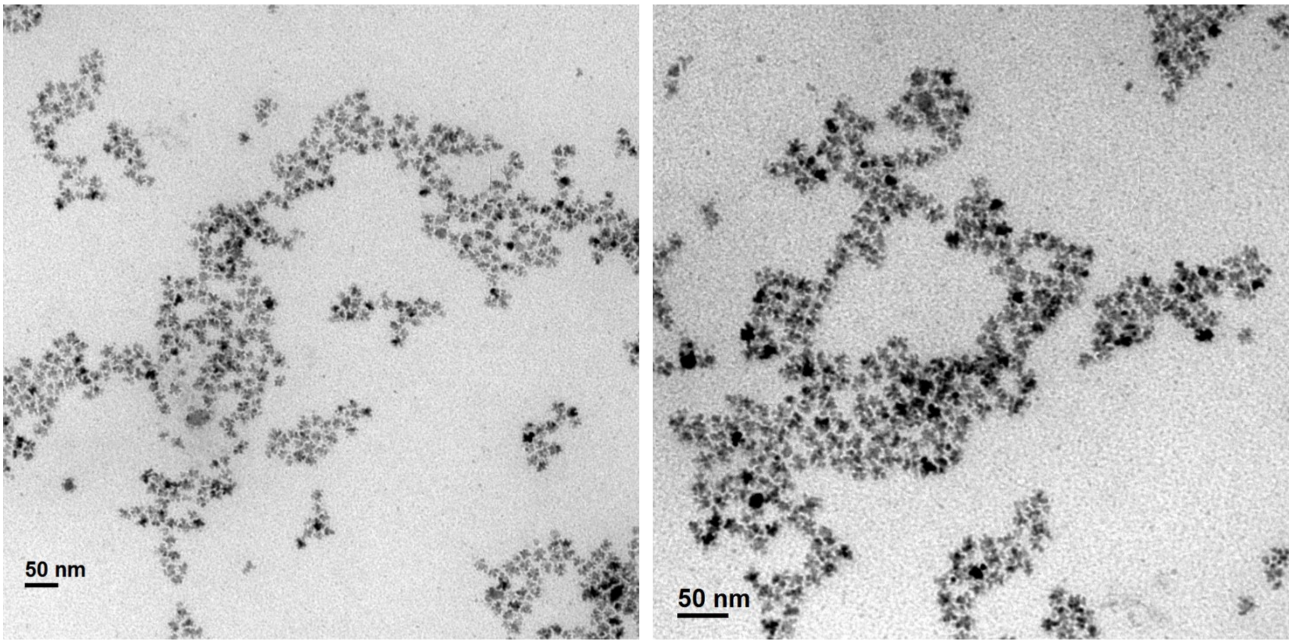

Figure S6. TEM micrographs of γ-Fe_2O_3@CoO NPs synthesized with a molar ratio OAc/Co = 8/1.

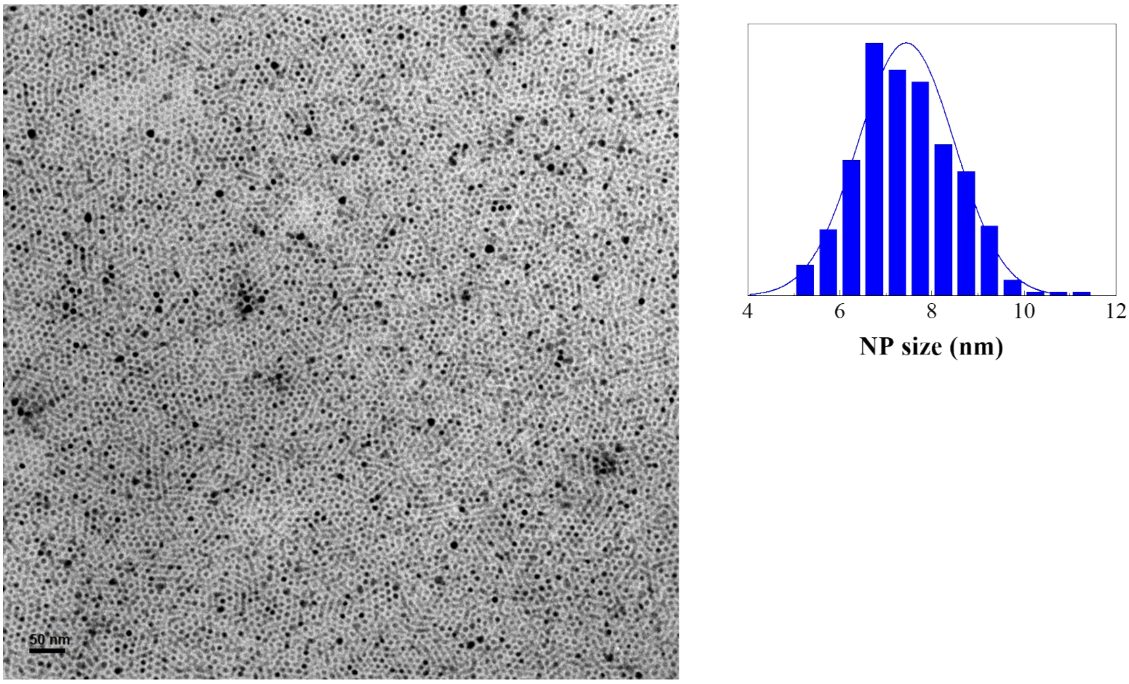

Figure S7. TEM micrograph and size distribution of cobalt oxide nanoparticles grown without the presence of iron oxide seeds with a molar ratio OAc/Co = 3/1.

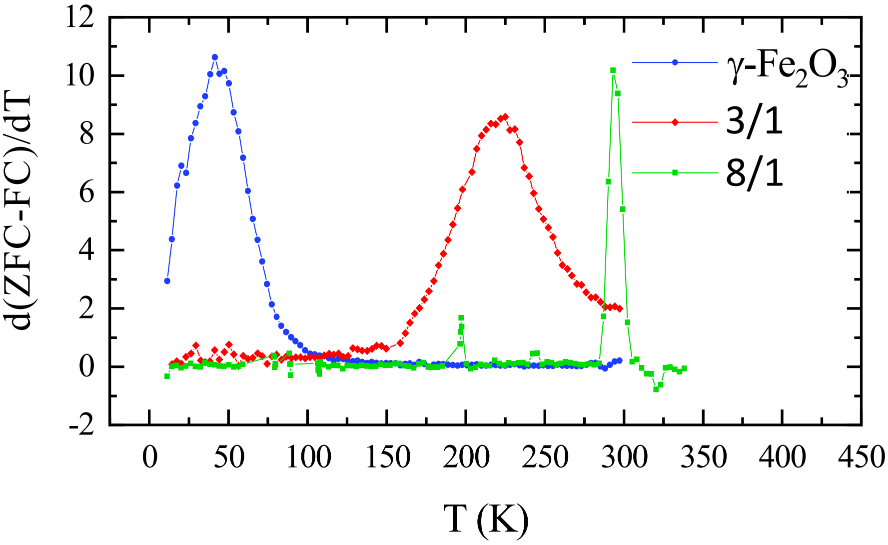

Figure S8. Derivative of ZFC measurements with temperature to obtain the average T_B for γ-Fe_2O_3 seeds and γ-Fe_2O_3 @CoO NP with molar ratios OAc/Co = 3/1 and 8/1.

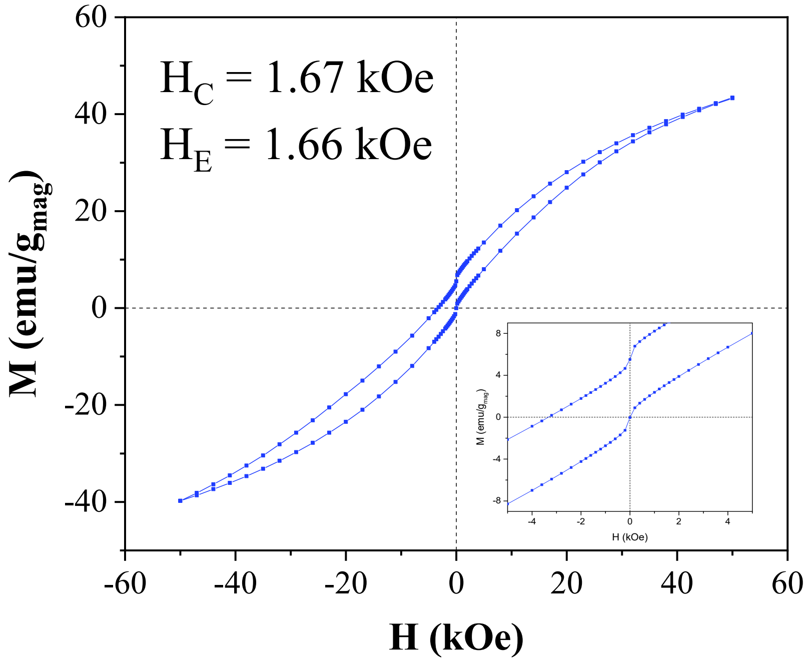

Figure S9. Hysteresis loop measured at 5 K after field-cooling (50 kOe) for γ-Fe_2O_3 @CoO NP with molar ratio OAc/Co = 3/1. Inset: Detail of the hysteresis loop when crossing the axes.

ICP-OES measurements were carried out for different OAc/Co ratios (Table S1). These values should be carefully analyzed. As remarked in the main manuscript, the size of the CoO satellites remains approximately constant (around 1-3 nm) independently of the amount of oleic acid. However, due to the small size and the proximity between cores and satellites, and also between adjacent satellites themselves, it is not possible to provide a more precise value. This can lead to a significant difference in mass (e.g. it is possible to have more satellites but slightly smaller in size thus influencing the final mass value).

In addition to previous considerations, the highest Co/Fe ratio (Table S1) is obtained with OAc/Co = 1/1. In this sample, as described in the main manuscript, some organic cloud-like features are still present (Fig. S2). Accordingly, the presence of cobalt associated with those organic regions (likely caused by a non-complete decomposition) cannot be ruled out, whether they are in the form of molecular complexes, small nuclei, clusters, or even as ultra-small particles of Co oxide that cannot be observed by TEM but would contribute to a higher Co/Fe ratio.

The Co/Fe ratios of samples with 3/1 and 5/1 are relatively similar. The advantage here in terms of accuracy is that both samples show a raspberry-like morphology with no presence of cloud-like features.

ICP measurements ran on the sample with OAC/Co molar ratio of 8/1 have led to a striking result. From the corresponding TEM micrograph (Fig. 2), it is evident that the sample has a high coverage of CoO outgrowths. However, although the coverage on the core by the satellites appears as more homogeneously distributed or denser than in the other samples, the size of the satellites is apparently smaller. As mentioned before, it is very difficult to ascertain which is their exact size in the approximate range of 1 to 3 nm, but they seem to be smaller than satellites in samples with OAc/Co molar ratio of 3/1 and 5/1, which could be the cause of the difference in the Co/Fe ratio (Table S1).

Table S1. Results from ICP-OES measurements for different OAc/Co ratios.

OAc/Co	**1/1**	**2/1**	**3/1**	**8/1**
[Fe] (g/L)	1.705	2.39	2.026	0.58
[Co] (g/L)	9.704	8.318	6.617	1.525
Co/Fe	5.691	3.480	3.266	2.629